Romanian Reports in Physics, Vol. 68, No. 3, P. 1170–1177, 2016

SYNTHESIS AND CHARACTERIZATION OF FLUORESCENT HYDROXYAPATITE

C.L. POPA[1], C.S. CIOBANU[1,2,*]

[1]National Institute of Materials Physics, P.O. Box MG 07, 07725, Magurele, Romania
[2]University Politehnica of Bucharest, Faculty of Applied Chemistry and Materials Science, Department of Science and Engineering of Oxide Materials and Nanomaterials, 1-7 Polizu Street, P.O. Box 12-134, 011061 Bucharest, Romania
*Corresponding author: ciobanu_carmen83@yahoo.com

Received July 1, 2015

Abstract. This paper presents the synthesis of cerium doped hydroxyapatite using low concentrations of cerium (x_{Ce} = 0.01, 0.03 and 0.05) by an adapted sol-gel method. The structural and optical properties of the obtained powders have been studied by X-Ray Diffraction (XRD), Fourier Transform Infrared Spectroscopy (FT-IR) and Photoluminescence (PL) measurements. The cerium ions successfully substituted the calcium ions from the hydroxyapatite structure without inflicting any structural alterations. With the increase of dopant concentration in the sample a decrease of the mean particle size was observed. Also, the vibrational peak intensities decreased while the intensity of the photoluminescence excitation bands increased in intensity when the cerium concentration increased from x_{Ce} = 0.01 to x_{Ce} = 0.05. Taken together, the results suggest that even low concentration of cerium influence the properties of hydroxyapatite but do not cause any structural alterations.

Key words: cerium, hydroxyapatite, structural and optical properties.

1. INTRODUCTION

The human bone matrix is formed of an organic part consisting of collagen fibers and an inorganic part consisting mainly of a biological mineral, hydroxyapatite [1–2]. Understanding the structure of the natural hard tissue is the first step in creating a synthetic replacement that could be used in orthopedic surgeries. Doctors and researchers alike have tried to find a substitute for the human bone due to the great number of orthopedic surgeries that involve the use of grafts or metallic implants. In this context, the field of tissue engineering (TE) has undergone a constant development in the last decades. Scientists involved in this kind of research have tried to create a synthetic material that could mimic the structure and properties of natural bone tissue, being able to facilitate the natural regeneration process [1, 3–5]. One of the most popular biomaterial used in many biomedical applications is hydroxyapatite (HAp). Due to its resemblance to the

inorganic component of bone and teeth, synthetic hydroxyapatite which has the chemical formula $Ca_{10}(OH)_2(PO_4)_6$ has already been used clinically as a coating material for metallic implants or as a remineralization material for dental enamel [6–8]. However, in spite of the fact that synthetic hydroxyapatite is very similar to the natural composite material, having outstanding properties such as an excellent bioactivity, biocompatibility and osteoconductivity [6, 9–10], it lacks the mechanical strength needed in heavy load-bearing applications [11] and the antibacterial properties [6, 12–14]. Therefore, scientists thought of improving the existing properties of HAp by substituting the Ca^{2+} ions from its structure with other metal ions which possess the properties that HAp requires in order to better fulfill its role as bone replacement material. In this context, researchers have focused on the rare earth elements, which are already being used in other fields, being constituents of permanent magnets, rechargeable batteries and catalysts [15]. Among the rare earth elements, much attention has been paid to cerium (Ce^{3+}) due to its antibacterial properties and its ability of preventing caries [6, 16–20]. Also, it has been used as a luminophor agent in the structure of ceramic powders in order to be used for dental applications because if the ceramic does not have fluorescent properties, it will have a grayish appearance which is not adequate in dentistry [21–22]. Furthermore, recent studies revealed that cerium has a beneficial effect on primary mouse osteoblasts *in vitro* while cerium oxide nanoparticles have the ability of acting as neuroprotective agents [23–25]. Moreover, it has already been demonstrated that cerium behaves similar to calcium in the human body, suggesting that compounds with Ce are able to stimulate the metabolism [26–28].

Due to the similar values of electronegativity and ionic radius between Ce and Ca, the replacement of Ca^{2+} ions by Ce^{3+} ions is possible. Therefore, the introduction of Ce ions in the lattice of HAp may improve the synthetic HAp by adding the properties of Ce to its already existing properties.

In this paper we report the synthesis of hydroxyapatite nanopowders doped with various concentration of cerium (x_{Ce} = 0.01, 0.03 and 0.05) by an adapted sol-gel method. The structural and optical properties of the obtained powders were also reported.

The obtained powders were investigated by X-ray diffraction (XRD), Fourier transform infrared spectroscopy (FTIR) and Photoluminescence (PL) measurements in order to obtain information about their structure and optical properties.

2. MATERIALS AND METHODS

2.1. SAMPLES

In this paper we report de preparation of Cerium doped hydroxyapatite (with chemical formula $Ca_{10-x}Ce_x(PO_4)_6(OH)_2$, [Ca + Ce]/P = 1.67) powders by an

adapted sol-gel method. The Cerium concentration used were: x_{Ce} = 0.01, 0.03 and 0.05. In order to obtain the Ce:HAp powders, an appropriate amount of P_2O_5 was added in an alcohol solution. Moreover, the $Ca(NO_3)_2 \cdot 4H_2O$ and $Ce(NO_3)_3 \cdot 6H_2O$ were also dissolved in absolute ethanol. The two solutions were mixed together under vigorous stirring for 1 day in order to obtain a gel. Afterwards, the gel was dried at 80°C for 24 h and ground thus obtaining the cerium doped hydroxyapatite nanopowder.

2.2. SAMPLE CHARACTERIZATION

X-Ray Diffraction (XRD). The X-ray diffraction patterns were recorded in the 2θ range 20^o–70^o using a Bruker D8 Advance diffractometer, with nickel filtered Cu K_α (λ = 1.5418 Å) radiation, and a high efficiency one-dimensional detector (Lynx Eye type) operated in integration mode.

Fourier Transform Infrared Spectroscopy (FTIR). The Fourier transform infrared spectroscopy (FTIR) studies have been performed using a Spectrum BX Spectrometer. The powders were prepared as follows: 1% of the powder was mixed with 99% KBr. The obtained mixture was pressed with a load of 5 tons for 2 min in order to obtain 10 mm diameter tablets. The spectrum was recorded in the 400 to 4000 cm^{-1} spectral region.

Photoluminescence (PL). The fluorescence emission spectra were obtained by using a HORIBA Scientific Fluorolog-3 spectrofluorometer (model FL3-2iHR320 with Hamamatsu R-928 PMT).

3. RESULTS AND DISCUSSIONS

Figure 1 shows the XRD patterns of the hydroxyapatite doped with various concentrations of cerium (x_{Ce} = 0.01, 0.03 and 0.05) (Ce:HAp) powders. From Fig. 1 we can see that the Ce:HAp samples exhibits diffraction peaks which are assigned to the characteristic plane of pure HAp with hexagonal structure. The diffraction patterns are in good agreement with the card (JCPDS No. 9-432). Moreover, other peaks associated with impurities have not been observed in any of the XRD patterns of Ce:HAp with x_{Ce} = 0.01, 0.03 and 0.05. The average crystal size of the synthesized Ce:HAp powders was determined by (211) peak broadening, using the Scherrer formula,

$$D = k\lambda/\beta\cos\theta,$$

where k is a constant chosen to be 0.9, λ is the wavelength of monochromatic X-ray beam equal to 0.15418 nm for CuK_α radiation, β is the full width at half maximum (FWHM) for the diffraction peak under consideration (in radians) and θ is the diffraction angle (^{o}). The particle size decreased when the concentration of

cerium increased. The average crystal size of Ce:HAp with x_{Ce} = 0.01 is 25.45 ± 0.1 nm while for Ce:HAp with x_{Ce} = 0.03 and x_{Ce} = 0.05 the crystal size (*D*) is 22.86 ± 0.1 nm and 18.95 ± 0.1 nm, respectively.

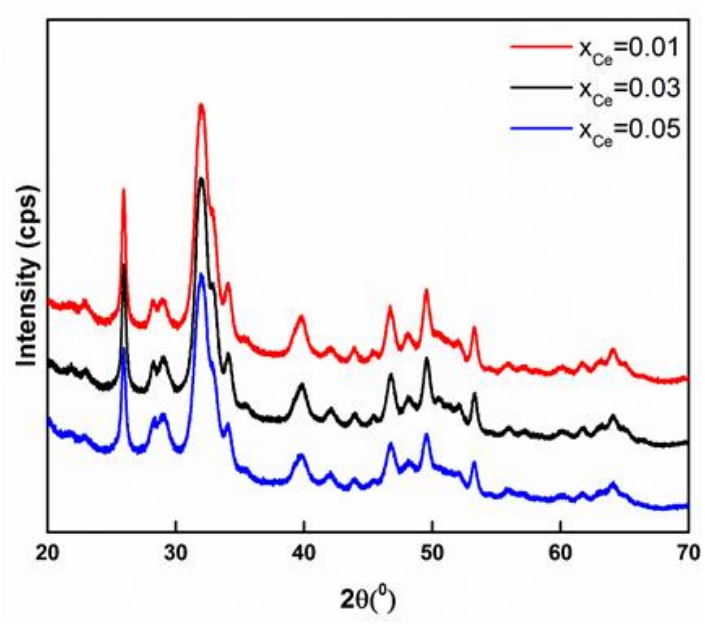

Fig. 1 – XRD patterns of Ce:HAp samples (x_{Ce} = 0.01, 0.03 and 0.05).

In Fig. 2 are presented the FT-IR deconvoluted spectra of cerium doped hydroxyapatite (x_{Ce} = 0.01, 0.03 and 0.05) in ν_4, ν_3, ν_2 and ν_1 regions of PO_4^{3-}. In order to obtain a satisfactory fit (for all the samples) seven components have been used in the spectral region of 450–700 cm^{-1}. The main vibrational bands presented in this region are attributed to ν_2 and ν_4 vibrations of PO_4^{3-} functional group. On the other hand, in the spectral region of 900–1200 cm^{-1} six components have been used in order to obtain a satisfactory fit. The bands observed in this region correspond to ν_1 and ν_3 vibrations of PO_4^{3-} group [29].

The main band presented in the ν_2 region is at 470 cm^{-1}. The bands associated to the ν_4 mode are identified at 566 and 602 cm^{-1}. The vibrational bands at around 960 cm^{-1} are attributed to ν_1 vibration of PO_4^{3-} group. Also, in the FTIR spectra were identified bands which correspond to ν_3 vibration of PO_4^{3-} group in the 1020–1140 cm^{-1} spectral region [30–35].

In addition, the presence of hydroxyapatite is proved by the presence of the band at around 630 cm^{-1} [30–32].

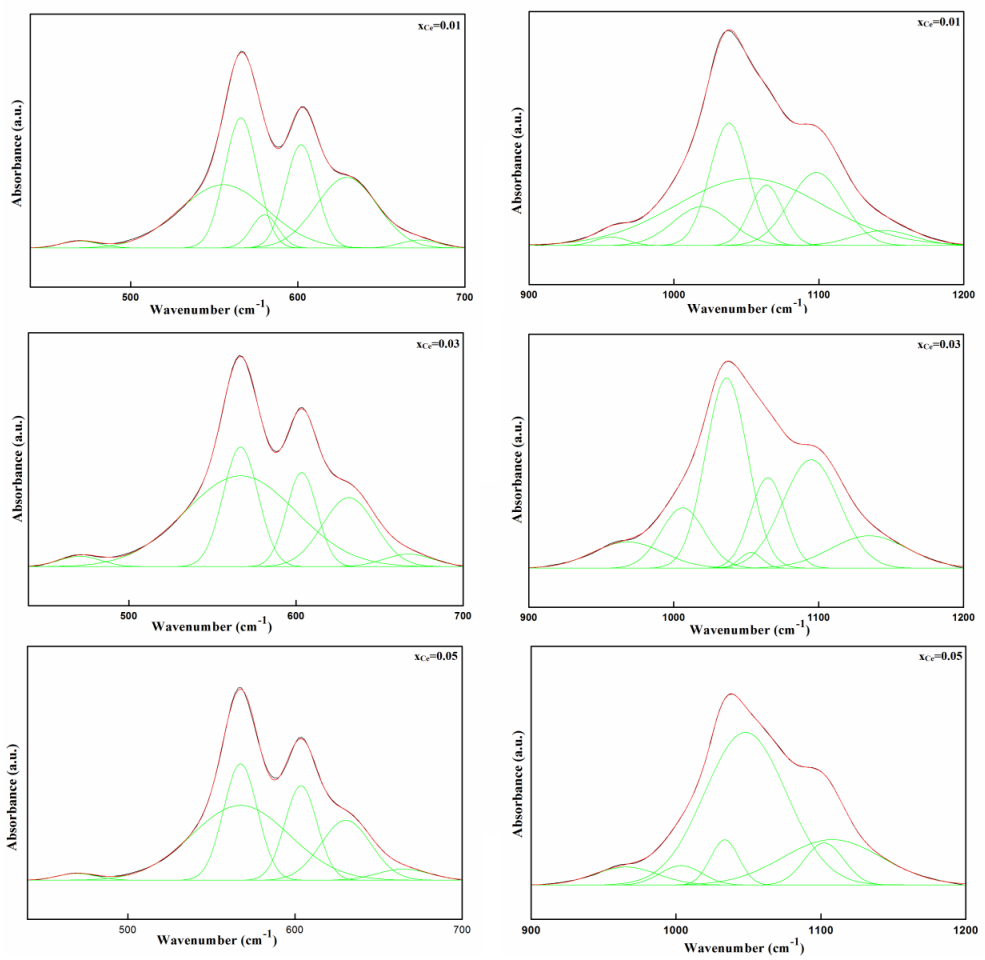

Fig. 2 – FTIR deconvoluted spectra of Ce:HAp powders
(with x_{Ce} = 0.01, 0.03 and 0.05).

It was noticed that the increase of cerium concentration in the samples leads to the decrease of the vibrational band intensity. It can also be observed that doping of the hydroxyapatite with cerium ions did not cause the appearance of any other additional vibrational bands associated with cerium or other impurities.

In Fig. 3 are presented the excitation spectra obtained for the Ce:HAp powders (λ_{em} = 385 nm). The excitations spectra exhibit one important band at 222 nm for Ce:HAp powders with x_{Ce} = 0.01, 224 nm for Ce:HAp powders with x_{Ce} = = 0.01 and at 226 nm for Ce:HAp powders with x_{Ce} = 0.05 respectively. This excitation band is assigned to the 5d-4f transitions of Ce^{3+} ions [36].

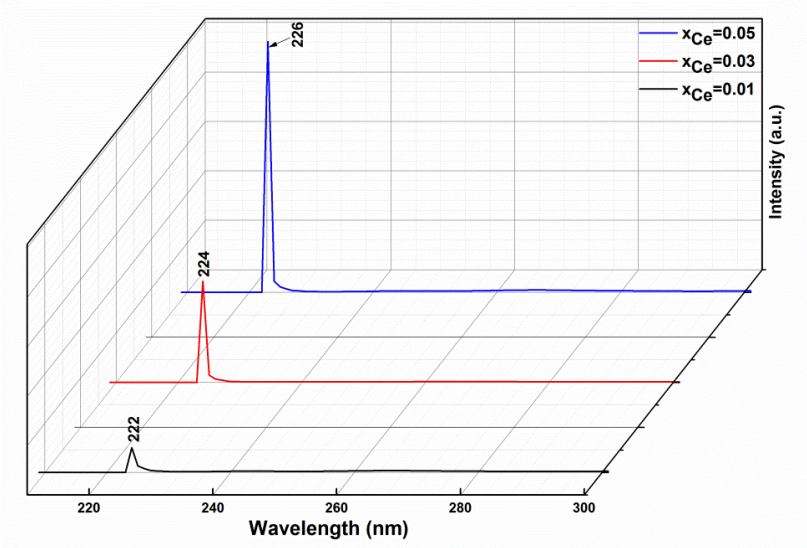

Fig. 3 – Excitation spectra of Ce:HAp (with x_{Ce} = 0.01, 0.03 and 0.05) powders (λ_{em}= 385 nm).

It is obvious that the intensity of the excitation band increases with the increase of Cerium concentration in the powders [37]. Moreover, in the excitation patterns it was observed the displacement of the excitation band with the increase of Ce in the samples [38–39].

The results reported in this paper shown the successful substitution of Ca^{2+} ions with Ce^{3+} ions in the hydroxyapatite structure. Moreover, the structural and optical properties of Ce:HAp powders were influenced by Cerium concentration.

4. CONCLUSIONS

The aim of our study was to obtain and to characterize cerium doped hydroxyapatite nanopowders with various concentration (x_{Ce} = 0.01, 0.03 and 0.05). The samples were synthesized by an adapted sol-gel method. The XRD investigations revealed that de average crystal size varies with cerium concentration. On the other hand, the intensity of vibrational bands decrease with the increase of cerium concentration in the samples. Moreover, it was noticed that the luminescence of the samples increases exponentially with the cerium concentration.

All the results presented in this paper confirm the successful substitution of Ca^{2+} ions with Ce^{3+} ions. Their integration in the hydroxyapatite matrix did not lead to any structural alteration, hexagonal HAp being the only phase found. However, the presence of the cerium ions causes the modification of the mean

crystal size, which decreases with the increase of cerium concentration, determines a decrease of the vibrational bands intensities in the FT-IR spectra and an increase of the PL excitation bands. It can be concluded that cerium present in the Ce:HAp samples alters, even at low concentrations, the properties of hydroxyapatite without modifying its structure.

This results confirm the formation of biocompatible fluorescent hydroxyapatite with controlled nanoscale particle size and a considerable capability for applications in various biomedical fields such as drug delivery and release or imaging and therapy.

Acknowledgements. The authors are grateful to Dr. Daniela Predoi (NIMP) for her contributions to this research. We thank HORIBA Scientific and especially Dr. Reynald HURTEAUX from Horiba Jobin Yvon SAS France for the access to their specific instrumentation. The work has been funded by the Sectoral Operational Programme Human Resources Development 2007–2013 of the Ministry of European Funds through the Financial Agreement POSDRU/159/1.5/S/134398.

REFERENCES

1. F. Sun, H. Zhou and J. Lee, Acta Biomater. **7**, 3813–3828 (2011).
2. P.K. Chu and X. Liu, *Biomaterials fabrication and processing handbook*, Boca Raton, FL, CRC Press, 2008.
3. A. Groza, Romanian Rep. Phys. **64**, 1227–1242 (2012).
4. A. Groza and A.Surmeian, J. Nanomater. **2015** 1–8 (2015).
5. A. Groza, A. Surmeian, C. Diplasu, M. Ganciu, Romanian Rep. Phys. **60**, 603–607 (2008).
6. L. Yingguang, Y. Zhuoru and C. Jiang, J. Rare Earth **25**, 452–456 (2007).
7. C. S. Ciobanu, A. Groza, S. L. Iconaru, C. L. Popa, P. Chapon, M. C. Chifiriuc, R. Hristu, G. A. Stanciu, C. C. Negrila, R. V. Ghita, M. Ganciu and D. Predoi, Biomed Res. Int., 2015, in press.
8. C. L. Popa, A. Groza, P. Chapon, C. S. Ciobanu, R. V. Ghita, R. Trusca, M. Ganciu and D. Predoi, J. Nanomater. **2015**, pp. 1–11 (2015).
9. Y. Wang, Y. Yan, M. Li and X. Jiang, J. Wuhan, Univ. Technol. – Mater Sci. Ed. **l8**, *1*, 33–36 (2003).
10. A. Hideki, *Science and Medical Applications of Hydroxyapatite*, Tokyo, JAAS, 1992.
11. H. Zhou and J. Lee, Acta Biomater. **7**, 2769–2781 (2011).
12. C.S. Ciobanu, C.L. Popa and D. Predoi, J. Nanomater. **2014**, 1–9 (2014).
13. A. Costescu, C. S. Ciobanu, S. L. Iconaru, R. V. Ghita, C. M. Chifiriuc, L. G. Marutescu, D. Predoi, J. Nanomater. **2013**, 1–9 (2013).
14. C. S. Ciobanu**,** F. Massuyeau**,** L. V. Constantin and D. Predoi, Nanoscale Res. Lett. **6**, 613 (2011).
15. C. E. Castano, M. J. O'Keefe, W. G. Fahrenholtz, Curr. Opin. Solid State Mater. Sci. **19**, 69–76 (2015).
16. J. Hemin, W. Xinqiang, L. Yongqian, L. Manqi, Y. Ke and Y. Zhiming, J. Chin. Rare Earth Soc. **24**, 223 (2006).
17. X. Liu and M. Tu, Modem Chemical Industry **25**, 145–147 (2005).
18. Yang Ling Mao Jim, Hou Tinghong *et al.*, New Chemical Materials **33**, 15 (2005).
19. G. Guaneheng, L. Duo, W. Zhihua and G. Hongyou, J. Rare Earth **23**, 362–366 (2005).
20. J. Hui, Z. Weipo and L. Huanhe, Chinese Journal of Stomatology **32**, 143 (1997).
21. O. Gunduz, C. Gode, Z. Ahmad, H. Gokce, M. Yetmez, C. Kalkandelen, Y.M. Sahin and F.N. Oktar, J. Mech. Behav. Biomed. Mater. **35**, 70–76 (2014).

22. C.A.M. Volpato, M.C. Fredel, A.G. Philippi and C.O. Petter, *Ceramic Materials and Colorin Dentistry*, in: *Wilfried Wunderlich Ceramic Materials Wilfried Wunderlich. Ceramic Materials and Colorin Dentistry*, 2010.
23. S. Shruti, A. J. Salinas, G. Lusvardi, G. Malavasi, L. Menabue and M. Vallet-Regi, Acta Biomater. **9**, 4836–4844 (2013).
24. Z. Jinchao, L. Cuilian, L. Yaping, S. Jing, W. Peng, D. Keqian *et al.*, *Effect of cerium ion on the proliferation, differentiation and mineralization function of primary mouse osteoblasts in vitro*, J Rare Earth **28**, 138–42 (2010).
25. D. Schubert, R. Dargusch, J. Raitano and S.W. Chan, Biochem. Biophys. Res. Commun. **342**, 86–91 (2006).
26. O. Kaygili, S. V. Dorozhkin and S. Keser, Mat. Sci. Eng. C **42**, 78–82 (2014).
27. J. Emsley, *Nature's Building Blocks: An A–Z Guide to the Elements*, Oxford University Press, 2011.
28. M.A. Jakupec, P. Unfried, B.K. Keppler, Rev. Physiol. Biochem. Pharmacol. **153**, 101–111(2005).
29. A. Groza, A. Surmeian, M. Ganciu, I.I. Popescu, Europhys. Lett. **68**, 652–657 (2004).
30. L. Berzina-Cimdina and N. Borodajenko, *Research of Calcium Phosphates Using Fourier Transform Infrared Spectroscopy, Infrared Spectroscopy – Materials Science, Engineering and Technology*, Prof. Theophanides Theophile (Ed.), 2012.
31. S. Koutsopoulos, J. Biomed. Mater. Res. **62**, 600–612 (2002).
32. C.S. Ciobanu, S.L. Iconaru, P. Le Coustumer, D. Predoi, J. Spectros., 1–5 (2013).
33. D. Predoi, Dig. J. Nanomater. Bios. **5**, 373–377 (2010).
34. D.Predoi and R.A. Vatasescu-Balcan, J. Optoelectron. Adv. M. **10**, 152–157 (2008).
35. D. Predoi, Dig. J. Nanomater. Bios. **2**, 169–173 (2007).
36. R. Ternane, M.Th. Cohen-Adad, G. Panczer, C. Goutaudier, C. Dujardin, G. Boulon, N. Kbir-Ariguib and M. Trabelsi-Ayedi, Solid State Sci. **4**, 53–59 (2002).
37. C.S. Ciobanu, S.L. Iconaru, F. Massuyeau, L.V. Constantin, A. Costescu and D. Predoi, J. Nanomater. **2012**, 1–9 (2012).
38. G.Q. Xu, Z.X. Zheng, W.M. Tang and Y.C. Wu, J. Lumin. **124**, 151–156 (2007).
39. W.M. Yen, S. Basun, U. Happek and M. Raukas, Acta. Phys. Pol. A **90** (1996).